Review Article

Ultra-precision valence electron density analysis: Unlocking quantum parameters with synchrotron X-ray diffraction

1. Introduction

Advances in synchrotron X-ray radiation has enabled previously challenging or impossible measurements, allowing refinement of numerous experimental techniques. This review explores the capabilities of X-ray diffraction, a fundamental application of synchrotron radiation.

Structural-property research elucidates physical properties through crystallographic information. While referencing crystal structures is standard in solid-state physics, recent advances in material synthesis have allowed precise structural control. Improved measurement techniques have also revealed unique physical phenomena that cannot be fully explained by conventional crystallographic data alone.

Band structure calculations are the primary approach used to understand physical properties and predict material behavior when accurate crystal structure data are available. However, for strongly correlated electron materials, where competing interactions exist, band calculations alone fail to capture the essential physics. First-principles calculations have expanded this approach, but inherent approximations and scalability issues sometimes yield contradictory results, particularly in time evolution via molecular dynamics and electronically excited states.

Experimental elucidation of electronic states thus remains crucial. While spectroscopic methods using synchrotron radiation have advanced [1,2], diffraction experiments still focus on powder diffraction and microcrystal analysis. High-precision single-crystal X-ray diffraction remains an underdeveloped approach in Japan. To address this, we introduced "ultra-precision analysis," which allows successful determination of quantum parameters from valence electron density (VED). This method enables experimental analysis even in high-temperature metastable states, paving the way for further advancements.

2. Investigating chemical bonding

Using the core-differential Fourier synthesis (CDFS) method, we successfully extracted only the VED within a crystal, which directly contributes to its physical properties. This method uses single-crystal X-ray diffraction data obtained from synchrotron radiation. A key advantage of our approach is that it does not require a quantum mechanical model, making it applicable to any single crystal approximately ten micrometers in size. The details of the analytical method have been described previously [3,4]. However, before delving into these specifics, we first introduce fundamental concepts of hybrid orbitals and chemical bonding, as described in textbooks, after which we explain high-resolution electronic orbital visualization and its physical implications to demonstrate the utility of our approach.

To investigate the σ-bonding in carbon–carbon interactions, we examined the glycine molecule, one of the simplest amino acids [5]. Figure 1(a) presents its structural formula alongside a conceptual representation of the surrounding electron cloud. The electron cloud's spatial distribution is described using the same conceptual framework as that for the bonding electron density in a hydrogen molecule. Figure 1(b) displays the experimentally obtained the VED distribution of crystalline glycine. Rather than having a smooth distribution, the VED is markedly inhomogeneous and discrete across the entire molecule. The cross-sectional view of the electron density (Fig. 1(c)) reveals distinct toroidal nodes (regions devoid of electron clouds) around carbon atoms C1 and C2, along with a significantly reduced electron density at the midpoint of the C1–C2 bond, where bonding orbitals are expected.

This seemingly counterintuitive pattern can be more clearly interpreted when considering that *sp* hybrid orbitals are formed by a combination of 2*s* and 2*p* orbitals. Unlike 1*s* orbitals, 2*s* orbitals, which possess a spherical distribution, exhibit nodal structures in the radial direction, resulting in a dual-shell configuration. This characteristic arises from the phase properties of the 2*s* orbital wave function. By experimentally identifying structural features of VED distributions, the wave functions that contribute to bond formation can be determined.

The experimentally obtained VED distribution aligned remarkably well with the results from long-range corrected-density functional theory. This agreement enabled distinction of orbital components within the

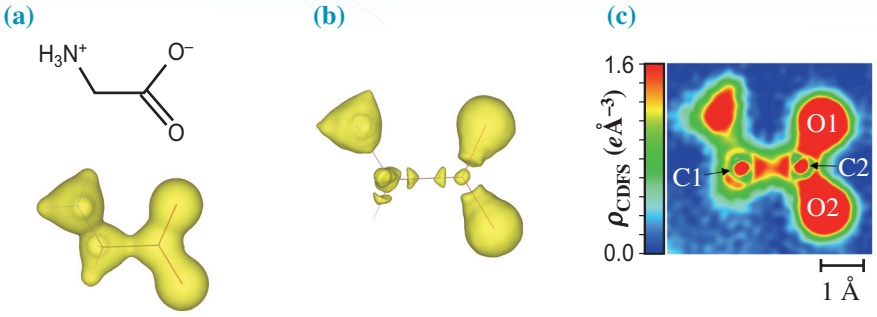

Fig. 1. Glycine: **(a)** chemical structure and an electron distribution model diagram drawn using the VESTA, **(b)** experimentally obtained valence electron density distribution, **(c)** cross-sectional view of the valence electron density.

VED by integrating experimental results with theoretical calculations. Consequently, we successfully visualized the distinctions between single and double bonds in chemical structures and captured the representation of π-electrons positioned above and below the plane of six-membered rings. This finding suggested the potential for directly applying molecular orbital concepts to molecular design in the field of chemistry.

3. Concepts of the core differential Fourier analysis method

To extract only the VED from diffraction data, we fully exploited the characteristics of atomic electron density distributions. As shown in Fig. 2, the atomic scattering factor for X-rays depends on the magnitude of the scattering vector, expressed as $\sin\theta/\lambda$, where λ is the X-ray wavelength and θ is the scattering angle. In conventional structural analysis, atomic scattering factors, based on the total electron density distribution of atoms, are used (black line). However, quantum mechanical computational methods enable the separation of contributions from inner-shell electrons (blue line) and valence electrons (orange line). Since inner-shell electrons are spatially confined, their contribution remains smooth, even at high scattering angles. In contrast, valence electrons exhibit a more extended spatial distribution and predominantly contribute to the low $\sin\theta/\lambda$ region. An important point is that the scattering factor of inner-shell electrons and the total atomic scattering factor almost overlap in the high-angle region.

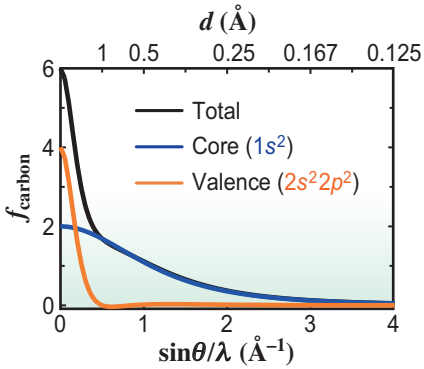

Fig. 2. Atomic scattering factor of carbon. The black line represents total electrons, the blue line corresponds to core-shell electrons ($1s^2$), and the orange line represents the valence electron components ($2s^22p^2$). The horizontal axis indicates the magnitude of the scattering vector, calculated from the X-ray wavelength (λ) and the scattering angle (θ).

Therefore, precise atomic positions can be determined using only high-angle X-ray diffraction data, which requires high-energy synchrotron X-rays. Based on this distribution, subtracting the contribution of the inner-shell electron density from the total X-ray diffraction measurements isolates the VED. The mathematical formulation of this process is detailed in Ref. [4], and a conceptual illustration is provided in Fig. 3. Consequently, to determine precise atomic positions (phase factors), refining the structure by using only high-angle X-ray diffraction data is sufficient. This principle underscores the advantage of high-energy X-rays for precise structural analysis, which is one of the key benefits of synchrotron X-rays.

Since VED information is crucial for understanding chemical bonding and physical properties, a fraction—approximately one-tenth to one-hundredth—of the total electron count of the chemical formula must be extracted. In terms of diffraction intensity, this corresponds to the square of these ratios. Consequently, stringent experimental constraints are imposed on the dynamic range, statistical precision, and spatial resolution of the diffraction intensities. If any of these conditions are not met, the reliability of the obtained information is severely compromised. High-quality synchrotron radiation X-rays, as quantum beams, play a crucial role in satisfying these stringent requirements. Further details on the beamline are described elsewhere [6].

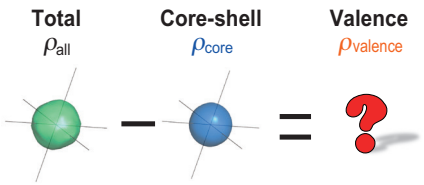

Fig. 3. Conceptual diagram of extracting only the valence electron density. Note that the total electron density distribution cannot be directly observed.

4. Observing 3*d* orbitals of transition metal at even higher resolution

By analyzing electron density using the CDFS method, we successfully observed σ bonds and double-bond states directly in small organic molecular crystals, demonstrating both the mechanism and reliability of this method. Nevertheless, extracting information that directly contributes to physical properties—such as the orbital degrees of freedom in transition metal oxides within strongly correlated electron systems—demands even higher spatial

resolution. Therefore, we attempted to observe the anisotropic 3*d* orbitals of a transition metal ion.

The target material for this study was the perovskite-type oxide $YTiO_3$, which has been extensively investigated as a standard material for orbital observation experiments since the 1970s (Fig. 4(a)). $YTiO_3$ is a Mott insulator in which the magnetic Ti^{3+} ion possesses 19 electrons, of which 18 inner-shell electrons form an overall isotropic spherical distribution and contribute minimally to its physical properties. The physical properties of the system are primarily governed by a single valence electron occupying the Ti 3*d* orbital. Due to the presence of a single electron in a doubly degenerate t_{2g} orbital, orbital degrees of freedom exist, and theoretical predictions suggest that electron correlation induces an antiferro-orbital ordered state (i.e., electrons at adjacent sites occupy different orbitals), resulting in ferromagnetism through the Kugel–Khomskii interaction.

Numerous experimental and theoretical studies have predicted the orbital state and the butterfly-shaped VED distribution, as shown in Fig. 4(b). The experimental details have been described previously [4]. Figure 4(c) presents the results of the CDFS analysis. The VED localized at the center of the TiO_6 octahedron clearly exhibits the butterfly-like shape of the 3*d* orbital, as depicted in quantum mechanics textbooks. This confirms the successful extraction of the VED distribution corresponding to the 3*d* orbital wave function without assuming any quantum mechanical model. Extracting quantum parameters of the 3*d* orbital from this anisotropic VED distribution yielded qualitative agreement with previous experimental and theoretical calculations, demonstrating that the quantum parameters of the Ti^{3+}: $3d^1$ orbital can be directly determined from the VED.

The relationship between the spatial resolution of the obtained diffraction data and the VED should also be considered. Figure 5 illustrates how the VED (cross-sectional view) changes with variation of the maximum scattering parameter $(\sin\theta/\lambda)_{max}$ used in the CDFS analysis. The X-ray diffraction data used for the CDFS analysis were identical in all aspects, except for the resolution. Figure 5(c), obtained using diffraction data with $(\sin\theta/\lambda)_{max}$ = 2.0 Å^{-1}, clearly reveals the anisotropy of the 3*d* orbital. However, the resolution of an X-ray diffraction apparatus using characteristic laboratory-based X-rays (Mo *K*α: λ = 0.71 Å) is limited to approximately $(\sin\theta/\lambda)_{max}$ ≈ 1.32 Å^{-1} (d_{min} ≈ 0.38 Å), preventing observation of orbital anisotropy. As previously mentioned, valence electron information is primarily contained in low-angle scattering intensities, but high-angle diffraction intensities are essential for accurately capturing the spatial anisotropy of VED.

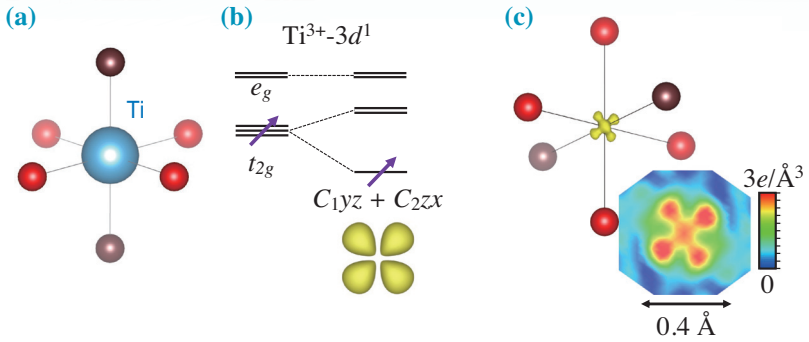

Fig. 4. **(a)** TiO_6 octahedron, **(b)** electron configuration of Ti^{3+}. Orbital degrees of freedom are lost due to both the distortion of the TiO_6 octahedron and electron correlation. **(c)** Experimentally obtained valence electron density distribution of Ti^{3+} [2].

5. Observing degenerate 3*d* orbitals

As noted earlier, several studies have reported the direct observation of orbital-ordered states. However, there remains a significant lack of research on the electron density observation of systems with orbital degrees of freedom, which are expected to exhibit strong responses to external fields. This study aims to investigate electron orbitals in which multiple electrons are localized within degenerate orbital states, without charge degrees of freedom, due to strong electron correlation.

The material investigated in this study, FeV_2O_4, has a spinel-type structure consisting of FeO_4 tetrahedra and VO_6 octahedra. In its high-temperature phase, it crystallizes in a cubic system with space group $Fd\bar{3}m$ (No. 227), exhibiting high symmetry. The formal valence states are Fe^{2+} and V^{3+}, corresponding to six and two 3*d* electrons, respectively. Due to the presence of geometric frustration in electronic correlations,

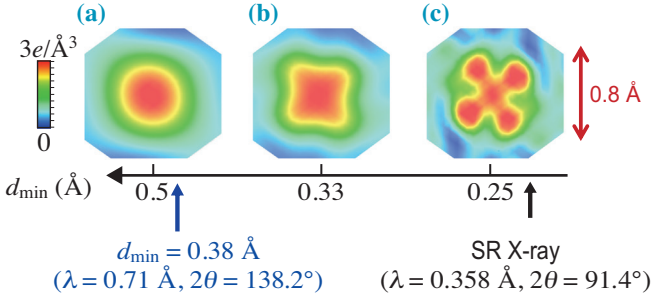

Fig. 5. Valence electron density distribution of Ti^{3+} with varying resolution. The same diffraction data were used for the CDFS analysis.

the spin, orbital, and lattice degrees of freedom are intricately intertwined, resulting in three structural and magnetic phase transitions upon cooling. Although various theoretical predictions have been made regarding the ground state, as discussed below, misinterpretations of the state with orbital degrees of freedom have hindered a full understanding.

For VO_6 octahedra at the V site in the cubic phase above 140 K, if a perfect octahedron is assumed, crystal field theory (O_h symmetry) predicts that the 3*d* orbitals would split into triply degenerate t_{2g} orbitals ($|yz\rangle$, $|zx\rangle$, $|xy\rangle$) and doubly degenerate e_g orbitals. The two 3*d* electrons of V^{3+} occupy the stabilized t_{2g} orbitals, preserving orbital degrees of freedom and leading to an expected $3d^2$ electron distribution (Fig. 6(a)). In the ground state, the system adopts tetragonal symmetry, and theoretical predictions suggest that a Jahn–Teller distortion along a specific axis would stabilize the electronic state, resulting in an orbital-ordered state.

However, the experimentally observed VED distribution of V^{3+} (Fig. 6(b)) exhibits pronounced anisotropy, indicating that the observed state is not a degenerate orbital state. This discrepancy arises because the VO_6 octahedra in the unit cell are not perfect octahedra. The site symmetry of V is $\bar{3}m$, possessing only a single, three-fold, improper rotation axis. Consequently, from a symmetry perspective, the octahedra are allowed to distort along the three-fold axis. Examination of the VO_6 octahedra within the unit cell confirms that they elongate along the $\langle 111 \rangle$ direction.

Under such D_{3d} distortion, the t_{2g} orbitals split into a doubly degenerate state and a singly occupied orbital. The quantization axis aligns with $\langle 111 \rangle$, uniquely determining the wave function of the singly occupied orbital, as shown in Fig. 6(c). The twofold degenerate orbitals remain undetermined, except for the condition that the three orbitals, including ϕ_1, must be mutually orthogonal. Consequently, even under D_{3d} distortion, the system retains orbital degeneracy.

The obtained VED distribution can be remarkably well explained by a model in which electrons probabilistically occupy ϕ_1 and the doubly degenerate orbitals. Further details are provided in the literature; however, this study represents the first direct observation clarifying how degenerate orbital electronic states manifest experimentally [7]. The theoretical predictions of the orbital ordering transition represent a typical case where the failure to account for the existence of ϕ_1 prevented reaching the correct conclusion.

6. Conclusion

As demonstrated above, this study introduced ultra-high-precision VED analysis using synchrotron radiation. Single-crystal diffraction experiments typically require various corrections, such as anisotropic absorption correction, multiple scattering, simultaneous reflection, and extinction effects. However, in practice, systematic errors arising from measurement conditions and detector characteristics often present more significant challenges. We successfully established a new analytical technique by using thorough adjustments and validations in collaboration with the facility staff. Our study demonstrated that by leveraging a high-quality X-ray source at SPring-8, qualitatively distinct analyses beyond conventional laboratory-based experiments can be achieved. As facilities and instrumentation continue to advance, the cutting-edge techniques described here may soon become standard methodologies. Furthermore, we are actively collaborating with synchrotron facilities to extend this VED observation method to operando measurements, accommodating multi-extreme conditions and external field responses.

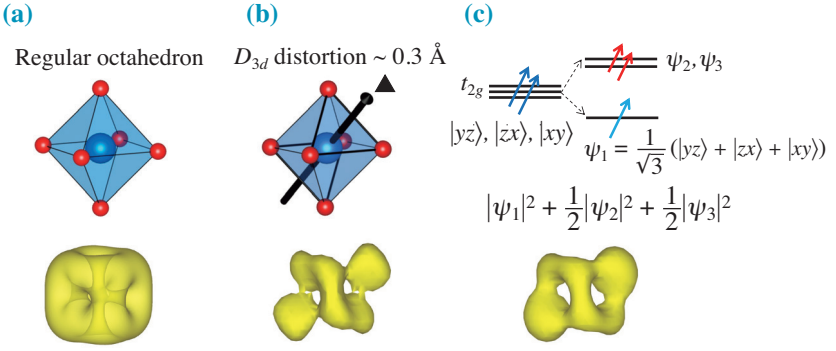

Fig. 6. Spinel structure FeV_2O_4 in the cubic phase $Fd\bar{3}m$: 3*d* orbital state of V^{3+} ($3d^2$: $S = 1$) in VO_6. **(a)** In the case of a regular octahedron, the 3*d* orbitals would be a cubic shape (simulation). **(b)** The VO_6 octahedron with D_{3d} distortion and an experimentally obtained valence electron density distribution. **(c)** Simulation results are estimated using quantum mechanical calculations with hydrogen-like wave functions.

Hiroshi Sawa†

Dept. Applied Physics, Nagoya University

Email: hiroshi.sawa@nagoya-u.jp

† Present address:
Nagoya Industrial Science Research Institute

References

[1] J. Itatani *et al.*: Nature **432** (2004) 213.
[2] H. Hafiz *et al.*: Nature **594** (2021) 213.
[3] S. Kitou *et al.*: Phys. Rev. Lett. **119** (2017) 065701.
[4] S. Kitou *et al.*: Phys. Rev. Res. **2** (2020) 033503.
[5] T. Hara *et al.*: J. Am. Chem. Soc. **146** (2024) 23825.
[6] K. Sugimoto *et al.*: AIP Conf. Proc. **1234** (2010) 887.
[7] T. Manjo *et al.*: Mater. Adv. **3** (2022) 3192.